

# High Performance Computing for Nanoplasmonic Laser Fusion

István Papp, Larissa Bravina, Mária Csete, Igor N. Mishustin, Dénes Molnár, Anton Motornenko, Leonid M. Satarov, Horst Stöcker, Daniel D. Strottman, András Szenes, Dávid Vass, Tamás S. Biró, László P. Csernai, Norbert Kroó



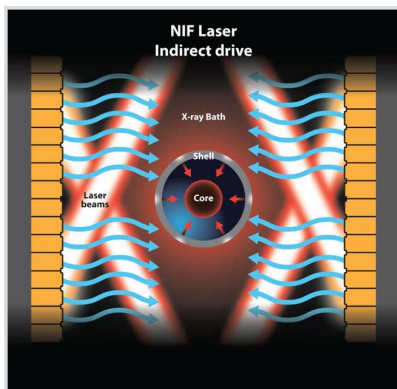
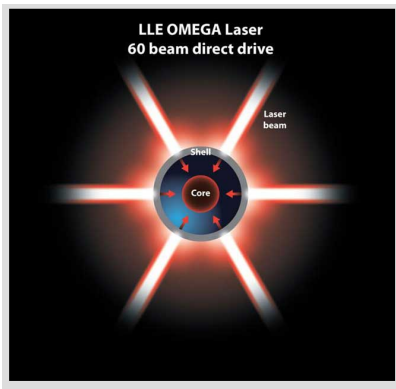
FIAS Frankfurt Institute  
for Advanced Studies



# Thermo-nuclear Fusion

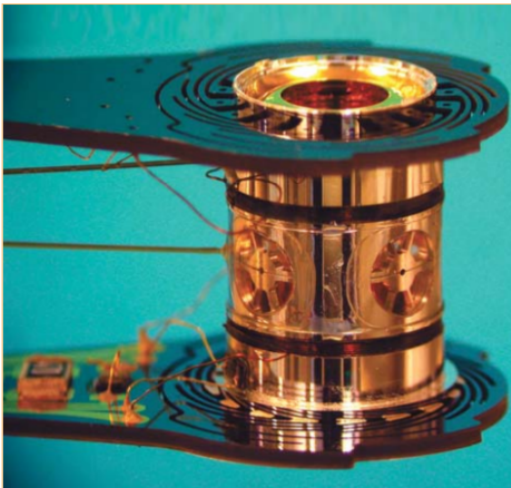
- Fusion does not happen spontaneously on Earth
- Total fusion energy  $E_f = \frac{1}{4}n^2\tau\epsilon\langle v\sigma\rangle$
- $\eta E_f$  is the usable energy
- The loss is  $(1 - \eta)(E_0 + E_b)$
- $E_0 = 3nkT$ ,  $E_b = bn^2\tau\sqrt{T}$  (thermal bremsstrahlung)
- Giving the gain factor:  $Q = \frac{\eta\epsilon n\tau v\sigma}{4(1-\eta)(3kT+bn\tau\sqrt{T})}$
- $Q$  must be  $Q > 1$  for energy production
- This also means  $n\tau > \frac{3kT(1-\eta)}{\frac{1}{4}\epsilon\eta\langle v\sigma\rangle - b(1-\eta)\sqrt{T}} \rightarrow \text{LC}$
- Fulfilling the Lawson criterion
  - Magnetically confined plasmas: increase confinement time
  - Inertial confinement fusion: increase density of fusion plasma

# Direct vs Indirect drive



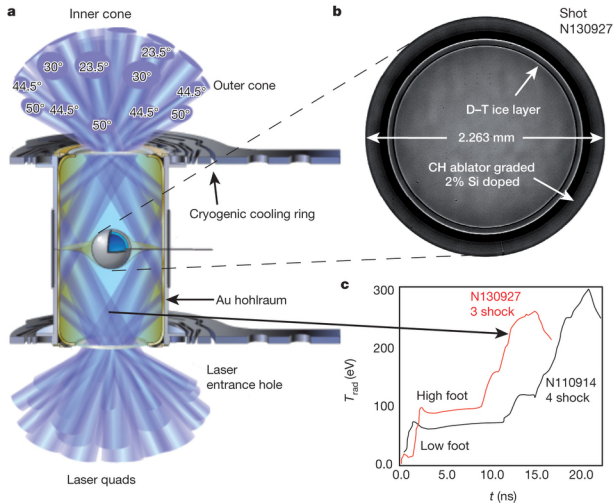
## Hohlraum 2014

LAWRENCE LIVERMORE NATIONAL LABORATORY



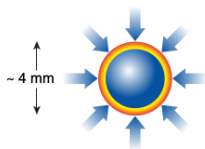
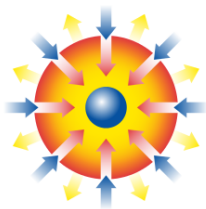
A **hohlraum** made from gold and 1 cm tall contains the fusion fuel capsule used in experiments at the National Ignition Facility. Light from the laser enters the ends of the cylinder and is converted to x rays, which implode the capsule.

## Hohlraum 2014

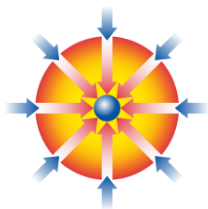
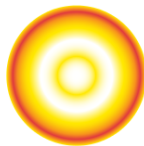


[O.A. Hurricane et al., Nature, 506, 343 (2014)]

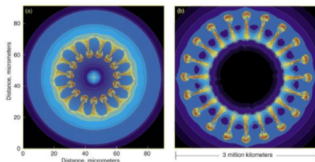
## Laser-Induced

Laser light shines  
on the targetThe target  
is compressed

The target is ignited

The target  
burns

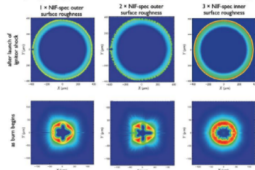
# Rayleigh-Taylor instabilities



Energy must be delivered as symmetric as possible!

Different levels of corrugation of the shell surfaces :

Striking similarities exist between hydrodynamic instabilities in (a) inertial confinement fusion capsule implosions and (b) core-collapse supernovae explosions. Image (a) is from Sakagami and Nishihara, *Physics of Fluids* #2, 2715 (1960); image (b) is from Hachisu et al., *Astrophysical Journal* 368, L27 (1991.)



**Left:** same roughness of inner and outer surface as specified for the NIF target

**Center:** outer surface roughness is twice the NIF level

**Right:** DT inner surface roughness three times larger than NIF specifications

[S. Atzeni et al., *Nucl. Fusion* 54, 054008 (2014).]

25

## RFD

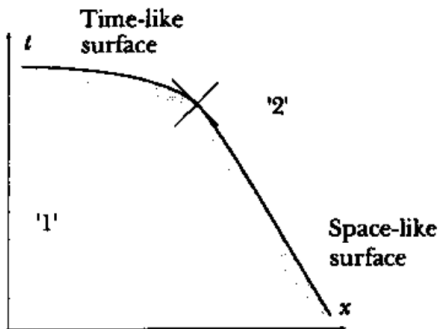


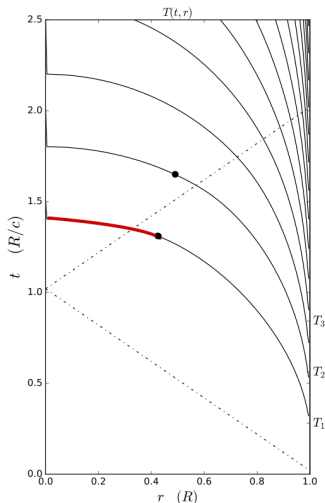
Figure 5.10: Smooth change from spacelike to timelike detonation  
[Csernai, L.P. (1987). Detonation on a time-like front for relativistic systems. Zh. Eksp. Teor. Fiz. 92, 379-386.]

## Constant absorptivity

[L.P. Csernai & D.D. Strottman, *Laser and Particle Beams* 33, 279 (2015)]

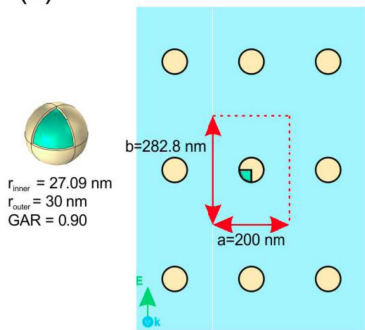
$$\alpha_{k_{middle}} = \alpha_{k_{edge}}$$

Simultaneous volume ignition is only up to 12%

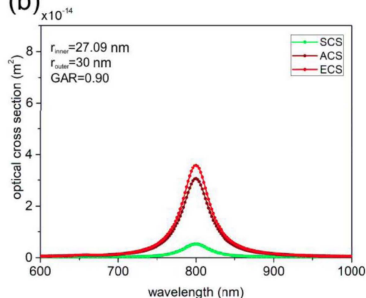


## Doping with gold

(a)



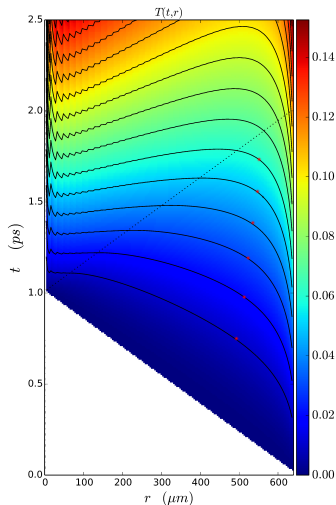
(b)



(a) Left: Single core-shell nano-sphere. Right: Rectangular lattice of nano-spheres in a transverse layer of the target.

(b) Optical cross-section of an individual core-shell nano-sphere optimized to absorb light at 800 nm wavelength and optical response of the same core-shell nano-spheres composing a rectangular lattice.

## Changing absorptivity

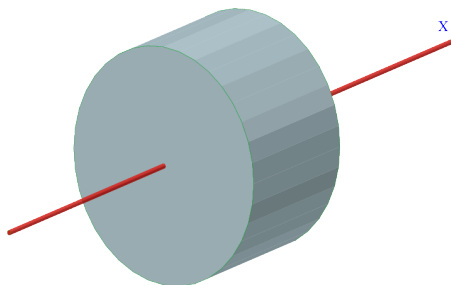


[Csernai, L.P., Kroo, N. and Papp, I. (2017). Procedure to improve the stability and efficiency of laser-fusion by nano-plasmonics method. Patent P1700278/3 of the Hungarian Intellectual Property Office.]

$$\alpha_{k_{middle}} \approx 4 \times \alpha_{k_{edge}}$$

Simultaneous volume ignition is up to 73%

## Flat target

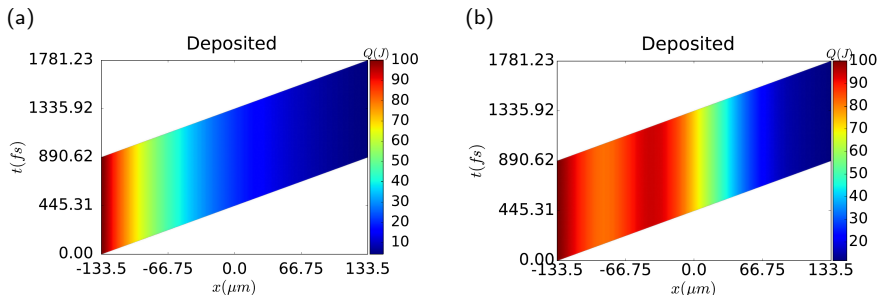


Schematic view of the cylindrical, flat target of radius,  $R$ , and thickness,  $h$ .

$$V = 2\pi R^3, \quad R = \sqrt[3]{V/(2\pi)}, \quad h = \sqrt[3]{4V/\pi}.$$

[L.P. Csernai, M. Csete, I.N. Mishustin, A. Motorenko, I. Papp, L.M. Satarov, H. Stcker & N. Kroó, Radiation- Dominated Implosion with Flat Target, *Physics and Wave Phenomena*, **28** (3) 187-199 (2020)]

## Varying absorptivity



**Deposited energy** per unit time in the space-time plane across the depth,  $h$ , of the flat target. **(a) without nano-shells (b) with nano-shells**

To increase central absorption we used the following distribution:

$$\alpha_{ns}(s) = \alpha_{ns}^C + \alpha_{ns}(0) \cdot \exp \left[ 4 \times \frac{\left(\frac{s}{100}\right)^2}{\left(\frac{s}{100} - 1\right) \left(\frac{s}{100} + 1\right)} \right].$$

# Similar configurations

Nuclear probes of an out-of-equilibrium plasma at the highest compression  
**Phys. Lett. A 383 (2019) 2285-2289.**

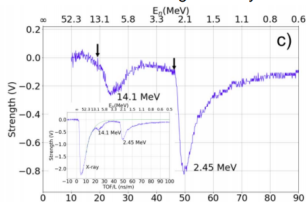
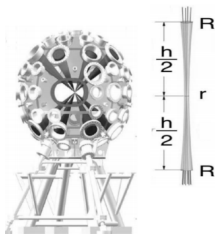
G. Zhang<sup>a,b,\*</sup>, M. Huang<sup>c</sup>, **A. Bonasera<sup>d,e,\*</sup>**, Y.G. Ma<sup>f,b,i,\*</sup>, B.F. Shen<sup>g,h,\*</sup>, H.W. Wang<sup>a,b</sup>,  
 W.P. Wang<sup>g</sup>, J.C. Xu<sup>g</sup>, G.T. Fan<sup>a,b</sup>, H.J. Fu<sup>b</sup>, H. Xue<sup>b</sup>, H. Zheng<sup>j</sup>, L.X. Liu<sup>a,b</sup>, S. Zhang<sup>c</sup>,  
 W.J. Li<sup>b</sup>, X.G. Cao<sup>a,b</sup>, X.G. Deng<sup>b</sup>, X.Y. Li<sup>b</sup>, Y.C. Liu<sup>b</sup>, Y. Yu<sup>g</sup>, Y. Zhang<sup>b</sup>, C.B. Fu<sup>k</sup>,  
 X.P. Zhang<sup>k</sup>

4 (up) + 4(down) lasers

Target thickness,  $h$  ( $3.6\mu\text{m}$ - $1\text{mm}$ )  
 & radius,  $R$ , ( $150$ - $400\mu\text{m}$ ) were varied.

Total pulse energy  $1.2\text{kJ}$  (2ns) for 8 beams.  
 Shortest (250ps) pulses  $\rightarrow$  100s MeV ions  $\rightarrow$   
 non-thermal distr. = directed ion acceleration

Typical fusion neutron energies were measured  
 & used to extract the target density.



33

# Similar configurations

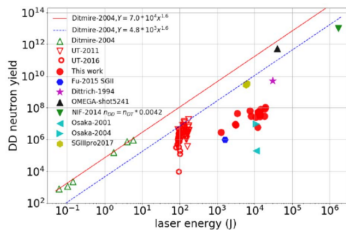


Figure 3: (color online) Fusion yield as function of laser energy. Different experimental results Ditmire-2004[40], UT-2011[20], UT-2016[19], Fu-2015 SGII[45], Dittrich-1994[49], NIF-2014[48], Osaka-2001[46], Osaka-2004[47], OMEGA-shot5241[41] and SGIIpro2017[42] are indicated in the inset.

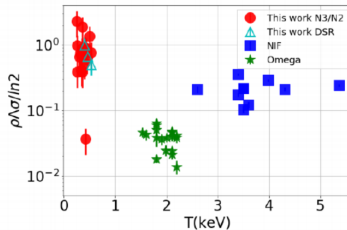
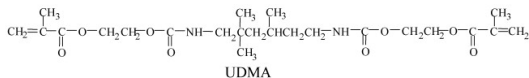
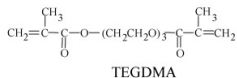
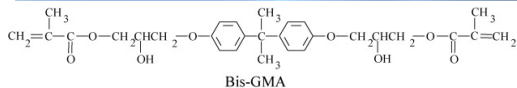


Figure 4: (color online)  $\Lambda \rho \sigma / \ln 2$  obtained from eq.(4) vs  $T$  from eq.(1). Omega and NIF data are derived from the experiments[25], using the Down Scatter Ratio[23, 21]. Our results using the DSR method ( $N_4/N_3$ ) are given by the open triangle symbols in good agreement with the  $N_3/N_2$  ratios.

# Experiment and collaboration



# Available software

Computational application	Web site	License	Availability	Canonical Reference
SHARP	[17]	Proprietary		doi:10.3847/1538-4357/aa6d13#
ALaDyn	[18]	GPLv3+	Open Repo:[19]	doi:10.5281/zenodo.49553#
<b>EPOCH</b>	[20]	GPL	Open to academic users but signup required [21]	doi:10.1088/0741-3335/57/11/113001#
FBPIC	[22]	3-Clause-BSD-LBNL	Open Repo:[23]	doi:10.1016/j.cpc.2016.02.007#
LSP	[24]	Proprietary	Available from ATK	doi:10.1016/S0168-9002(01)00024-9#
MAGIC	[25]	Proprietary	Available from ATK	doi:10.1016/0010-4655(95)00010-D#
OSIRIS	[26]	Proprietary	Closed (Collaborators with MoU)	doi:10.1007/3-540-47789-6_36#
<b>PICCANTE</b>	[27]	GPLv3+	Open Repo:[28]	doi:10.5281/zenodo.48703#
PICLas	[29]	Proprietary	Available from Institute of Space Systems# and Institute of Aerodynamics and Gas Dynamics# at the University of Stuttgart	doi:10.1016/j.crme.2014.07.005#
PIConGPU	[30]	GPLv3+	Open Repo:[31]	doi:10.1145/2503210.2504564#
SMILEI	[32]	CeCILL-B	Open Repo:[33]	doi:10.1016/j.cpc.2017.09.024#
iPIC3D	[34]	Apache License 2.0	Open Repo:[35]	doi:10.1016/j.matcom.2009.08.038#
The Virtual Laser Plasma Library	[36]	Proprietary	Unknown	doi:10.1017/S0022377899007515#
VizGrain	[37]	Proprietary	Commercially available from Esgee Technologies Inc.	
VPIC	[38]	3-Clause-BSD	Open Repo:[39]	doi:10.1063/1.2840133#
VSIm (Vorpal)	[40]	Proprietary	Available from Tech-X Corporation	doi:10.1016/j.jcp.2003.11.004#
Warp	[41]	3-Clause-BSD-LBNL	Open Repo:[42]	doi:10.1063/1.860024#
WarpX	[43]	3-Clause-BSD-LBNL	Open Repo:[44]	doi:10.1016/j.nima.2018.01.035#
ZPIC	[45]	AGPLv3+	Open Repo:[46]	

# Particle In Cell methods

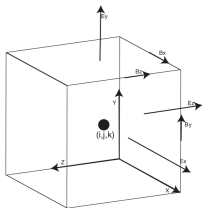


Figure 1. Yee staggered grid used for the Maxwell solver in EPOCH.

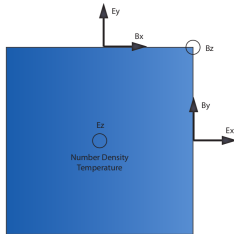


Figure 2: The Yee grid in 2D

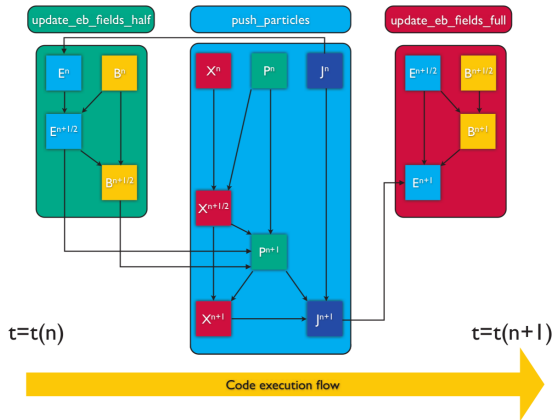
[T.D. Arber et al 2015 Plasma Phys. Control. Fusion 57 113001]

A **super-particle (marker-particle)** is a computational particle that represents many real particles.

Particle **move** or **pusher** algorithm as standard **Boris algorithm**.

**Finite-difference time-domain method** for solving the time evolution of **Maxwell's equations**.

## General layout of the EPOCH code



[EPOCH 4.0 dev manual]

- (input) deck
- housekeeping
- io
- parser
- physics\_packages
- user\_interaction

## FDTD in EPOCH

- $\mathbf{E}_{n+\frac{1}{2}} = \mathbf{E}_n + \frac{\Delta t}{2} \left( c^2 \nabla \times \mathbf{B}_n - \frac{\mathbf{j}_n}{\epsilon_0} \right)$
- $\mathbf{B}_{n+\frac{1}{2}} = \mathbf{B}_n - \frac{\Delta t}{2} \left( \nabla \times \mathbf{E}_{n+\frac{1}{2}} \right)$
- Call particle pusher which calculates  $\mathbf{j}_{n+1}$
- $\mathbf{B}_{n+1} = \mathbf{B}_{n+\frac{1}{2}} - \frac{\Delta t}{2} \left( \nabla \times \mathbf{E}_{n+\frac{1}{2}} \right)$
- $\mathbf{E}_{n+1} = \mathbf{E}_{n+\frac{1}{2}} + \frac{\Delta t}{2} \left( c^2 \nabla \times \mathbf{B}_{n+1} - \frac{\mathbf{j}_{n+1}}{\epsilon_0} \right)$

## Particle pusher

- Solves the relativistic equation of motion under the Lorentz force for each marker-particle

$$\mathbf{p}_{n+1} = \mathbf{p}_n + q\Delta t \left[ \mathbf{E}_{n+\frac{1}{2}}(\mathbf{x}_{n+\frac{1}{2}}) + \mathbf{v}_{n+\frac{1}{2}} \times \mathbf{B}_{n+\frac{1}{2}}(\mathbf{x}_{n+\frac{1}{2}}) \right]$$

$\mathbf{p}$  is the particle momentum  $q$  is the particle's charge  $\mathbf{v}$  is the velocity.

$\mathbf{p} = \gamma m \mathbf{v}$ , where  $m$  is the rest mass  $\gamma = [(\mathbf{p}/mc)^2 + 1]^{1/2}$

- Villasenor and Buneman current deposition scheme [Villasenor J & Buneman O 1992 Comput. Phys. Commun. 69 306], always satisfied:  $\nabla \cdot \mathbf{E} = \rho/\epsilon_0$ , where  $\rho$  is the charge density.

## Particle shape

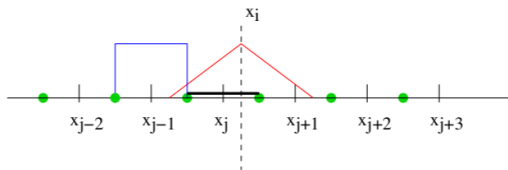


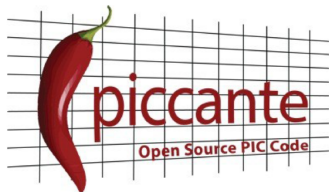
Figure 3: Second order particle shape function

First order approximations are considered

$$F_{part} = \frac{1}{2} F_{i-1} \left( \frac{1}{2} + \frac{x_i - X}{\Delta x} \right)^2 + \frac{1}{2} F_i \left( \frac{3}{4} - \frac{(x_i - X)^2}{\Delta x^2} \right)^2 + \frac{1}{2} F_{i+1} \left( \frac{1}{2} + \frac{x_i - X}{\Delta x} \right)^2$$

[EPOCH 4.0 dev manual]

# A spicy code

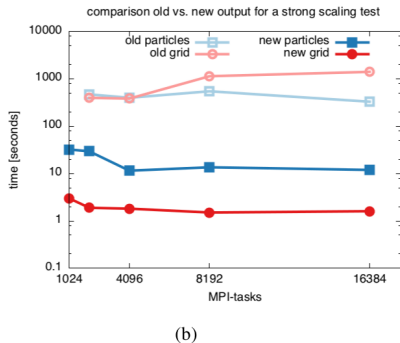
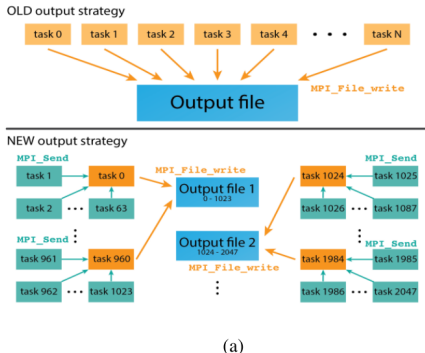


Still beta version Supports:

- rough\_box features
- grating
- grid stretching
- highly optimized output

- 1 A. Sgattoni, et. al., Laser-Driven Rayleigh-Taylor Instability: Plasmonics Effects and Three-Dimensional Structures, Phys. Rev. E, 91, 013106 (2015)
- 2 A. Sgattoni, et. al., High Energy Gain in Three-Dimensional Simulations of Light Sail Acceleration, Appl. Phys. Lett., 105, 084105 (2014)
- 3 L. Fedeli, et. al., Electron acceleration by relativistic surface plasmons in laser-grating interaction, Physical Review Letters 116, 015001 (2016)
- 4 A. Sgattoni, et. al., High field plasmonics and laser-plasma acceleration in solid targets, Plasma Physics and Controlled Fusion 58, 014004 (2015)

# Benefits of a spicy code



(a) Old and new strategies.  $G = 64$  group of tasks and  $F = N/128$  master tasks.

(b) Time spent for **writing particle positions** red, time spent for **grid based outputs** (EM fields, densities) marked with blue.

# Ionisation

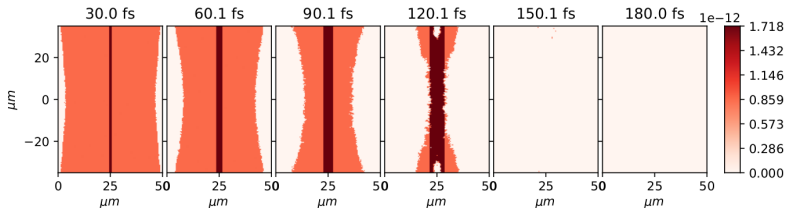


Figure 2: (color online) The ionization of the  $H$  atoms in a Laser Wake Field (LWF) wave due to the irradiation from both the  $\pm x$ - directions, on an initial target density of  $n_H = 2.13 \cdot 10^{27}$  atoms/m<sup>3</sup> =  $2.13 \cdot 10^{21}$  atoms/cm<sup>3</sup>. The energy of the  $H$  atoms in Joule [J] per marker particle is shown. The  $H$  atoms disappear as protons and electrons are created. Due to the initial momentum of the colliding  $H$  slabs, the target and projectile slabs interpenetrate each other and this leads to double energy density. Several time-steps are shown at 30 fs time difference.

However **PICCANTE** does **not** contain ionisation

**EPOCH** **includes** a number of ionisation models by which electrons ionise in both the field of an intense laser and through collisions.

[Keldysh L 1965 Sov. Phys.JETP 20 1307]

## Conclusions, Looking forward

- Mechanical, pressure driven processes are subject to RT instability, while shorter and more energetic irradiation can prevent the possibility of all mechanical instabilities.
- For more realistic estimates relativistic analysis is needed
- First steps include only smaller lasers with monomer targets
- PICCANTE unfinished, but with essential advantages
- For experimental physicists EPOCH is more user friendly